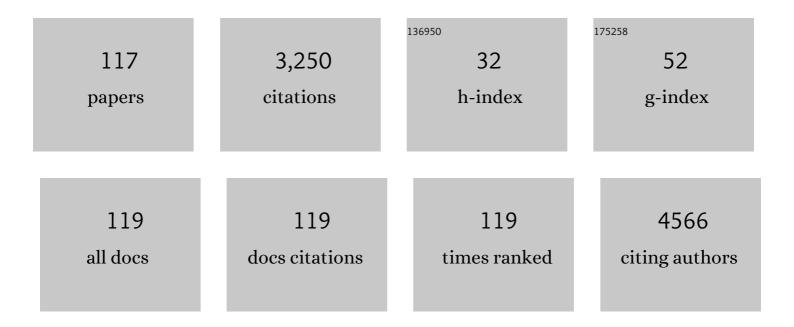
List of Publications by Year in descending order

Source: https://exaly.com/author-pdf/1720089/publications.pdf Version: 2024-02-01



ACHICH CADC

#	Article	IF	CITATIONS
1	Low-Temperature Microwave Processed TiO ₂ as an Electron Transport Layer for Enhanced Performance and Atmospheric Stability in Planar Perovskite Solar Cells. ACS Applied Energy Materials, 2022, 5, 2679-2696.	5.1	11
2	Rapid Involution of Large Cardiac Rhabdomyomas With Everolimus Therapy. World Journal for Pediatric & Congenital Heart Surgery, 2021, 12, 426-429.	0.8	12
3	Role of PC60BM in defect passivation and improving degradation behaviour in planar perovskite solar cells. Solar Energy Materials and Solar Cells, 2020, 207, 110335.	6.2	23
4	Temperature dependent Xâ€ray diffraction and Raman spectroscopy studies of polycrystalline YCrO 3 ceramics across the T C ~ 460 K. Journal of Raman Spectroscopy, 2020, 51, 537-545.	2.5	10
5	Probing the Interface Activation in Designing Defect-Free Multilayered Polymer Nanocomposites for Dielectric Capacitor Applications. Journal of Physical Chemistry C, 2020, 124, 22914-22924.	3.1	18
6	Establishment of Myocardial Strain Measurement Data in Pediatric Patients Without Structural Heart Disease: A Single Center Study. Pediatric Cardiology, 2020, 41, 892-898.	1.3	6
7	Improved ferroelectric response of pulsed laser deposited BiFeO3-PbTiO3 thin films around morphotropic phase boundary with interfacial PbTiO3 buffer layer. Journal of Applied Physics, 2020, 127, .	2.5	12
8	Poly(vinylpyrrolidone)/Poly(vinylidene fluoride) as Guest/Host Polymer Blends: Understanding the Role of Compositional Transformation on Nanoscale Dielectric Behavior through a Simple Solution–Process Route. ACS Applied Energy Materials, 2019, 2, 6146-6152.	5.1	38
9	Maghemite/Polyvinylidene Fluoride Nanocomposite for Transparent, Flexible Triboelectric Nanogenerator and Noncontact Magneto-Triboelectric Nanogenerator. ACS Sustainable Chemistry and Engineering, 2019, 7, 14856-14866.	6.7	26
10	Dicyanovinylene and Thiazolo[5,4- <i>d</i>]thiazole Core Containing D–A–D Type Hole-Transporting Materials for Spiro-OMeTAD-Free Perovskite Solar Cell Applications with Superior Atmospheric Stability. ACS Applied Energy Materials, 2019, 2, 7609-7618.	5.1	26
11	Temperature dependent structural and electrical analysis of Cr-doped multiferroic GaFeO ₃ ceramics. Materials Research Express, 2019, 6, 115704.	1.6	3
12	Thiazolothiazoleâ€Based Fluorescence Probe towards Detection of Copper and Iron Ions through Formation of Radical Cations. ChemistrySelect, 2019, 4, 11718-11725.	1.5	20
13	Multifunctional and Flexible Polymeric Nanocomposite Films with Improved Ferroelectric and Piezoelectric Properties for Energy Generation Devices. ACS Applied Energy Materials, 2019, 2, 6364-6374.	5.1	52
14	Enhanced efficiency and thermal stability of mesoscopic perovskite solar cells by adding PC70BM acceptor. Solar Energy Materials and Solar Cells, 2019, 202, 110130.	6.2	23
15	Milli-Watt Power Harvesting from Dual Triboelectric and Piezoelectric Effects of Multifunctional Green and Robust Reduced Graphene Oxide/P(VDF-TrFE) Composite Flexible Films. ACS Applied Materials & Interfaces, 2019, 11, 38177-38189.	8.0	56
16	Does myocardial strain remain abnormal long after normalization of ejection fraction in patients with acute myocarditis?. Echocardiography, 2019, 36, 609-612.	0.9	3
17	Control of electrical leakage in magnetoâ€electric gallium ferrite via aliovalent substitution. Journal of the American Ceramic Society, 2019, 102, 7414-7427.	3.8	5
18	Significantly Enhanced Energy Density by Tailoring the Interface in Hierarchically Structured TiO ₂ –BaTiO ₃ –TiO ₂ Nanofillers in PVDF-Based Thin-Film Polymer Nanocomposites. ACS Applied Materials & Interfaces, 2019, 11, 14329-14339.	8.0	121

#	Article	IF	CITATIONS
19	Engineered thiol anchored Au-BaTiO3/PVDF polymer nanocomposite as efficient dielectric for electricnic applications. Composites Science and Technology, 2019, 174, 158-168.	7.8	89
20	Origin of ferroelectricity in orthorhombic <mml:math xmlns:mml="http://www.w3.org/1998/Math/MathML"><mml:msub><mml:mi mathvariant="normal">LuFeO<mml:mn>3</mml:mn></mml:mi </mml:msub>. Physical Review B, 2019, 100, .</mml:math 	3.2	14
21	Impedance spectroscopy on degradation analysis of polymer/fullerene solar cells. Solar Energy, 2019, 178, 133-141.	6.1	30
22	Modeling of degradation in normal and inverted OSC devices. Solar Energy Materials and Solar Cells, 2019, 191, 329-338.	6.2	7
23	Flexible and Robust Piezoelectric Polymer Nanocomposites Based Energy Harvesters. ACS Applied Materials & Interfaces, 2018, 10, 2793-2800.	8.0	100
24	Organic solar cells on Al electroded opaque substrates: Assessing the need of ZnO as electron transport layer. Solar Energy, 2018, 160, 396-403.	6.1	16
25	Electrical and impedance spectroscopy analysis of sol-gel derived spin coated Cu2ZnSnS4 solar cell. Journal of Applied Physics, 2018, 123, .	2.5	34
26	Screen printed PEDOT:PSS films as transparent electrode and its application in organic solar cells on opaque substrates. Journal of Materials Science: Materials in Electronics, 2018, 29, 11030-11038.	2.2	16
27	A fluorene-core-based electron acceptor for fullerene-free BHJ organic solar cells—towards power conversion efficiencies over 10%. Chemical Communications, 2018, 54, 4001-4004.	4.1	26
28	Nd and Ru co-doped bismuth titanate polycrystalline thin films with improved ferroelectric properties. Journal Physics D: Applied Physics, 2018, 51, 055301.	2.8	4
29	Effect of sintering temperature on structure and properties of GaFeO3. Journal of Alloys and Compounds, 2018, 737, 646-654.	5.5	15
30	Effect of tantalum doping in a TiO ₂ compact layer on the performance of planar spiro-OMeTAD free perovskite solar cells. Journal of Materials Chemistry A, 2018, 6, 1037-1047.	10.3	86
31	Effect of Zn doping on structural and ferroelectric properties of GaFeO <inf>3</inf> for futuristic spintronic applications. , 2018, , .		0
32	Study of structural and magnetic characterization of polycrystalline Y0.5Ho0.5CrO3. AIP Conference Proceedings, 2018, , .	0.4	0
33	National Survey of Pediatric Care Providers: Assessing Time and Impact of Coding and Documentation in Physician Practice. Clinical Pediatrics, 2018, 57, 1300-1303.	0.8	8
34	It Is Not Always Sepsis: Fatal Tachypnea in a Newborn. Case Reports in Pediatrics, 2018, 2018, 1-3.	0.4	3
35	Incidence and factors influencing the spontaneous closure of Fontan fenestration. Congenital Heart Disease, 2018, 13, 776-781.	0.2	9
36	Progress in tailoring perovskite based solar cells through compositional engineering: Materials properties, photovoltaic performance and critical issues. Materials Today Energy, 2018, 9, 440-486.	4.7	58

#	Article	IF	CITATIONS
37	Synthesis, growth, and characterizations of CuO single crystal. AIP Conference Proceedings, 2018, , .	0.4	3
38	Dielectric relaxation and ac conductivity in magnetoelectric YCrO3 ceramics: A temperature dependent impedance spectroscopy analysis. Journal of the European Ceramic Society, 2018, 38, 5359-5366.	5.7	23
39	Unilateral lung agenesis, hiatal hernia and atrioventricular septal defect: a rare combination of congenital anomalies. BMJ Case Reports, 2018, 2018, bcr-2018-224382.	0.5	1
40	Sr and Mn co-doped sol-gel derived BiFeO ₃ ceramics with enhanced magnetism and reduced leakage current. Materials Research Express, 2017, 4, 015702.	1.6	33
41	An efficient route to fabricate fatigue-free P(VDF-TrFE) capacitors with enhanced piezoelectric and ferroelectric properties and excellent thermal stability for sensing and memory applications. Physical Chemistry Chemical Physics, 2017, 19, 7743-7750.	2.8	24
42	Modifications of the structure and magnetic properties of ceramic YCrO ₃ with Fe/Ni doping. Materials Research Express, 2017, 4, 076104.	1.6	20
43	Temperature and grain size effect on electrical properties of gallium ferrite polycrystalline ceramic. AIP Conference Proceedings, 2017, , .	0.4	2
44	Room temperature multiferroism in polycrystalline thin films of gallium ferrite. Journal of Alloys and Compounds, 2017, 721, 593-599.	5.5	12
45	Synthesis of a NbO Type Homochiral Cu(II) Metal–Organic Framework: Ferroelectric Behavior and Heterogeneous Catalysis of Three-Component Coupling and Pechmann Reactions. Inorganic Chemistry, 2017, 56, 4697-4705.	4.0	42
46	Solutionâ€Processed Organic Solar Cells Using New Electron Acceptor Derived from Naphthalene and Fluorene Unit. ChemistrySelect, 2017, 2, 7913-7917.	1.5	4
47	Effect of annealing atmosphere on leakage and dielectric characteristics of multiferroic gallium ferrite. Journal of the American Ceramic Society, 2017, 100, 5226-5238.	3.8	34
48	Significant reduction in the leakage current of Cr-doped GaFeO3 synthesized by sol–gel method. Applied Physics A: Materials Science and Processing, 2017, 123, 1.	2.3	13
49	One-Step Synthesis of New Electron Acceptor for High Efficiency Solution Processable Organic Solar Cells. Journal of Physical Chemistry C, 2017, 121, 26615-26621.	3.1	11
50	Temperature dependent electron paramagnetic resonance study on magnetoelectric YCrO ₃ . Journal of Physics Condensed Matter, 2017, 29, 495805.	1.8	14
51	Inkjet printing of NiO films and integration as hole transporting layers in polymer solar cells. Scientific Reports, 2017, 7, 1775.	3.3	41
52	A Rare Adrenal Mass in a 3-Month-Old: A Case Report and Literature Review. Case Reports in Pediatrics, 2017, 2017, 1-5.	0.4	6
53	The combined effect of mechanical strain and electric field cycling on the ferroelectric performance of P(VDF-TrFE) thin films on flexible substrates and underlying mechanisms. Physical Chemistry Chemical Physics, 2016, 18, 29478-29485.	2.8	11
54	High temperature X-ray diffraction, Raman spectroscopy and dielectric studies on yttrium orthochromites. AIP Conference Proceedings, 2016, , .	0.4	3

#	Article	IF	CITATIONS
55	Pediatric Resident Attitudes and Knowledge of Critical Congenital Heart Disease Screening. Pediatric Cardiology, 2016, 37, 1137-1140.	1.3	4
56	Inverted polymer bulk heterojunction solar cells with ink-jet printed electron transport and active layers. Organic Electronics, 2016, 35, 118-127.	2.6	16
57	Inverted P3HT:PCBM organic solar cells on low carbon steel substrates. Solar Energy, 2016, 133, 339-348.	6.1	17
58	Buffer layers in inverted organic solar cells and their impact on the interface and device characteristics: An experimental and modeling analysis. Organic Electronics, 2016, 37, 228-238.	2.6	14
59	Spin phonon interactions and magnetodielectric effects in multiferroic BiFeO ₃ –PbTiO ₃ . Journal of Physics Condensed Matter, 2016, 28, 075901.	1.8	26
60	Ferroelectric polarization switching with a remarkably high activation energy in orthorhombic GaFeO3 thin films. NPG Asia Materials, 2016, 8, e242-e242.	7.9	72
61	Composition-dependent structural and Raman spectroscopic studies on Y1-xHoxCrO3 (0≤â‰0.1). AIP Conference Proceedings, 2015, , .	0.4	2
62	Electrical and magnetic characterization of multiferroic BiFeO3-PbTiO3 thin films. AIP Conference Proceedings, 2015, , .	0.4	1
63	Effect of isovalent non-magnetic Fe-site doping on the electronic structure and spontaneous polarization of BiFeO3. Journal of Applied Physics, 2015, 117, 184104.	2.5	11
64	Metal–Organic Frameworks Built from a Linear Rigid Dicarboxylate and Different Colinkers: Trap of the Keto Form of Ethylacetoacetate, Luminescence and Ferroelectric Studies. Crystal Growth and Design, 2015, 15, 4526-4535.	3.0	29
65	Microscopic Investigations into the Effect of Surface Treatment of Cathode and Electron Transport Layer on the Performance of Inverted Organic Solar Cells. ACS Applied Materials & Interfaces, 2015, 7, 16418-16427.	8.0	19
66	Enhancement in magnetic properties of Ba-doped BiFeO 3 ceramics byÂmechanical activation. Journal of Alloys and Compounds, 2015, 651, 294-301.	5.5	27
67	Understanding the formation of PEDOT:PSS films by ink-jet printing for organic solar cell applications. RSC Advances, 2015, 5, 78677-78685.	3.6	45
68	Improved lifetimes of organic solar cells with solutionâ€processed molybdenum oxide anodeâ€modifying layers. Progress in Photovoltaics: Research and Applications, 2015, 23, 989-996.	8.1	22
69	Aging and memory effect in magnetoelectric gallium ferrite single crystals. Journal of Magnetism and Magnetic Materials, 2015, 375, 49-53.	2.3	9
70	Suppression of grain boundary relaxation in Zr-doped BiFeO3 thin films. Journal of Applied Physics, 2014, 115, .	2.5	14
71	Interface morphology driven control of electrical properties of P(VDF–TrFE) and PMMA blend M–l–M capacitors. Organic Electronics, 2014, 15, 3811-3817.	2.6	10
72	Structure and Properties of Magnetoelectric Gallium Ferrite: A Brief Review. Ferroelectrics, 2014, 473, 154-170.	0.6	9

#	Article	IF	CITATIONS
73	Structural investigation of multiferroic BiFeO3-PbTiO3 solid solution. , 2014, , .		1
74	Optical anisotropy in bismuth titanate: An experimental and theoretical study. Journal of Applied Physics, 2014, 115, 133509.	2.5	3
75	Phonons and magnetic excitation correlations in weak ferromagnetic YCrO3. Journal of Applied Physics, 2014, 115, .	2.5	57
76	A novel 3D 10-fold interpenetrated homochiral coordination polymer: large spontaneous polarization, dielectric loss and emission studies. CrystEngComm, 2014, 16, 4766.	2.6	18
77	Cooling rate controlled microstructure evolution and reduced coercivity in P(VDF–TrFE) devices for memory applications. Organic Electronics, 2014, 15, 82-90.	2.6	19
78	Large ferroelectric polarization of chemical solution processed BiFeO3–PbTiO3 thin films. Solid State Communications, 2014, 177, 103-107.	1.9	9
79	Electrophoretic deposition of nanocrystalline hydroxyapatite on Ti6Al4V/TiO2 substrate. Journal of Coatings Technology Research, 2013, 10, 263-275.	2.5	15
80	Room Temperature Nanoscale Ferroelectricity in MagnetoelectricGaFeO3Epitaxial Thin Films. Physical Review Letters, 2013, 111, 087601.	7.8	99
81	Engineering polarization rotation in ferroelectric bismuth titanate. Applied Physics Letters, 2013, 102, .	3.3	12
82	Understanding the role of thickness and morphology of the constituent layers on the performance of inverted organic solar cells. Solar Energy Materials and Solar Cells, 2013, 116, 135-143.	6.2	45
83	Dielectric response and magnetoelectric coupling in single crystal gallium ferrite. AIP Advances, 2013, 3, .	1.3	17
84	Microstructure and interfacial chemistry of pure and La-doped BiFeO3thin films. Microscopy Research and Technique, 2013, 76, 1304-1309.	2.2	0
85	Thin film transistors fabricated by evaporating pentacene under electric field. Journal of Applied Physics, 2013, 114, 154517.	2.5	17
86	Understanding degradation mechanism of bulk heterojunction organic photovoltaic devices. , 2012, , .		0
87	Spin glass-like phase below â^¼210 K in magnetoelectric gallium ferrite. Applied Physics Letters, 2012, 100, 112904.	3.3	43
88	Effect of site-disorder on magnetism and magneto-structural coupling in gallium ferrite: A first-principles study. Journal of Applied Physics, 2012, 111, .	2.5	16
89	Inkjet printed PEDOT:PSS for organic devices. , 2012, , .		2
90	Effects of site disorder, off-stoichiometry and epitaxial strain on the optical properties of magnetoelectric gallium ferrite. Journal of Physics Condensed Matter, 2012, 24, 435501.	1.8	14

#	Article	IF	CITATIONS
91	Multiferroic Memories. Advances in Condensed Matter Physics, 2012, 2012, 1-12.	1.1	96
92	Compositional dependence of structural parameters, polyhedral distortion and magnetic properties of gallium ferrite. Solid State Communications, 2012, 152, 1181-1185.	1.9	48
93	Quasi-Cubic Magnetite/Silica Core-Shell Nanoparticles as Enhanced MRI Contrast Agents for Cancer Imaging. PLoS ONE, 2011, 6, e21857.	2.5	58
94	Probing magnetoelastic coupling and structural changes in magnetoelectric gallium ferrite. Journal of Physics Condensed Matter, 2011, 23, 445403.	1.8	45
95	Absence of morphotropic phase boundary effects inÂBiFeO3–PbTiO3 thin films grown via a chemical multilayer deposition method. Applied Physics A: Materials Science and Processing, 2011, 104, 395-400.	2.3	17
96	An investigation in InGaO3(ZnO)m pellets as cause of variability in thin film transistor characteristics. Bulletin of Materials Science, 2011, 34, 447-454.	1.7	5
97	Electronic structure, Born effective charges and spontaneous polarization in magnetoelectric gallium ferrite. Journal of Physics Condensed Matter, 2011, 23, 325902.	1.8	39
98	Influence of Zr doping on the structure and ferroelectric properties of BiFeO3 thin films. Journal of Applied Physics, 2010, 107, .	2.5	74
99	First-principles calculations of Born effective charges and spontaneous polarization of ferroelectric bismuth titanate. Journal of Physics Condensed Matter, 2010, 22, 165902.	1.8	27
100	Structural changes and ferroelectric properties of BiFeO3–PbTiO3 thin films grown via a chemical multilayer deposition method. Journal of Applied Physics, 2009, 105, .	2.5	24
101	Photovoltaic effect in arylenevinylene-co-pyrrolenevinylene (AVPV). Solar Energy Materials and Solar Cells, 2009, 93, 211-214.	6.2	3
102	BiFeO3 ceramics synthesized by mechanical activation assisted versus conventional solid-state-reaction process: A comparative study. Journal of Alloys and Compounds, 2009, 477, 780-784.	5.5	102
103	Impedance spectroscopy studies on polycrystalline BiFeO3 thin films on Pt/Si substrates. Journal of Applied Physics, 2009, 105, .	2.5	85
104	Magnetic studies of multiferroic Bi _{1â^'<i>x</i>} FeO ₃ ceramics synthesized by mechanical activation assisted processes. Journal of Physics Condensed Matter, 2009, 21, 026007.	1.8	62
105	Effect of cooling conditions on the magnetic structure of multiferroic BiFeO3 synthesized by mechanical activation. Hyperfine Interactions, 2008, 187, 81-86.	0.5	1
106	Phase stability in ferroelectric bismuth titanate: a first-principles study. Acta Crystallographica Section A: Foundations and Advances, 2008, 64, 368-375.	0.3	33
107	Structural, dielectric and ferroelectric study of Ba0.9Sr0.1ZrxTi1â~'xO3 ceramics prepared by the sol–gel method. Physica B: Condensed Matter, 2008, 403, 1819-1823.	2.7	64
108	Phase evolution, magnetic and electrical properties in Sm-doped bismuth ferrite. Journal of Applied Physics, 2008, 103, .	2.5	156

#	Article	IF	CITATIONS
109	Comparative wear performance of titanium based coatings for automotive applications using exhaust gas recirculation. Surface and Coatings Technology, 2007, 201, 6182-6188.	4.8	12
110	Development of high strength hydroxyapatite by solid-state-sintering process. Ceramics International, 2007, 33, 419-426.	4.8	249
111	Novel Low-Temperature Synthesis of Ferroelectric Neodymium-Doped Bismuth Titanate Nanoparticles. Journal of the American Ceramic Society, 2007, 90, 1295-1298.	3.8	7
112	DEPOSITION AND CHARACTERIZATION OF PULSED-LASER-DEPOSITED AND CHEMICAL-SOLUTION-DERIVED SM-SUBSTITUTED BISMUTH TITANATE FILMS. Integrated Ferroelectrics, 2006, 79, 113-121.	0.7	0
113	Preliminary Investigation Into Comparative Performance of Titanium Based Coatings for Automotive Applications Using Biodiesel Blend and Diesel. , 2006, , .		0
114	Growth and characterization of pulsed-laser-deposited polycrystalline Bi3.33Sm0.67Ti3O12 ferroelectric thin films. Materials Letters, 2005, 59, 2583-2587.	2.6	3
115	Structural and electrical properties of samarium-substituted bismuth titanate ferroelectric thin films on Pt/TiOx/SiO2/Si substrates. Thin Solid Films, 2005, 484, 188-195.	1.8	19
116	Pulsed Laser Deposition of Epitaxial SrBi 2 Ta 2 O 9 Films with Controlled Orientation. Ferroelectrics, 2002, 268, 89-94.	0.6	2
117	Epitaxial Growth of Fully a -/ b -axis Oriented SrBi 2 Ta 2 O 9 Films. Integrated Ferroelectrics, 2002, 44, 1-8.	0.7	3